Chiang Mai J. Sci. 2018; 45(3) : 1486-1498
http://epg.science.cmu.ac.th/ejournal/
Contributed Paper

Achieving Adsorption of Cationic Dyes by the Composites Based on $H_3PMo_{12}O_{40}$ Decorating Metal Organic Frameworks

Wenpeng Gong, Xiaogang Du, Xiaoxia Liu, Xiaofen Ke and Shuijin Yang*
Hubei Collaborative Innovation Center for Rare Metal Chemistry, Hubei Key Laboratory of Pollutant Analysis & Reuse Technology, College of Chemistry and Chemical Engineering, Hubei Normal University, Huangshi 435002, China.
* Author for correspondence; e-mail: yangshuijin@163.com

Received: 26 September 2016
Accepted: 9 March 2017

ABSTRACT

The novel $H_3PMo_{12}O_{40}$/MOF-5($Zn_4O(BDC)_3$) adsorbent has been prepared by hydrothermal synthetic method with $H_3PMo_{12}O_{40}$ and metal-organic frameworks (MOF-5) as materials active species and supports, respectively. The composition, structure, morphology, stability and toleration of $H_3PMo_{12}O_{40}$/MOF-5 have been characterized through X-ray powder diffraction pattern (XRD), Fourier transform infrared spectrum (FT-IR), scanning electron micrographs (SEM), thermogravimetric (TG), brunaue Emmett teller (BET). The adsorption of methylene blue onto $H_3PMo_{12}O_{40}$/MOF-5 in aqueous solution was studied. The effects of the experimental parameters, including sample solution initial pH, temperature and initial concentration have been investigated. The results showed that the lower temperature and lower pH value were beneficial to the dye adsorption. The experiment data could be well described by the Langmuir equations and pseudo-sencond-order kinetic model. Thermodynamic parametars $\Delta G<0$, $\Delta H<0$ and $\Delta S>0$ indicated that the MB adsorption onto $H_3PMo_{12}O_{40}$/MOF-5 was spontaneous and endothermic, the adsorption towards methyl violet, rhodamine B and malachite green cationic dyes also showed good adsorption properties. The quite efficient adsorption of cationic dyes in aqueous solution on $H_3PMo_{12}O_{40}$/MOF-5 was studied.

Keywords: adsorption, cationic dyes, $H_3PMo_{12}O_{40}$, metal organic frameworks

1. INTRODUCTION

The continuous development of society promotes the chemical industry's development, at the same time accompanied by an increasing number of industrial waste water, one of the main hazardous industrial waste water is dyeing waste water, which has become one of the major sources of pollution. At present, the production of dyestuff has reached one million tons, and it's widely used in the textile, paint, food technology and hair dyeing process [1-2] and so on. The processing methods such as discharge has caused immeasurable threat to the environment and human health, due to

their highly visibility and undesirability even at a small amount ,their toxicity and carcinogennicity[3],as well as stable to light.

So it is urgent to use different sewage treatment technology to deal with different kinds of dye waste water so as to realize sewage discharging standard or recycling. In recent years, domestic and foreign chemical workers have made great efforts to search for novel and effective technique to eliminate of hazardous dyes from aqueous solution, until now, many methods such as electrochemical water treatment technology[4],physical, chemical, biological methods and photocatalytic degradation [5] have been investigated. The adsorption method has gradually attracted great research interest, which is regarded as a very important technique, due to its high efficiency along with low cost and simplicity of operation. Therefore, looking for a kind of effective adsorption material is crucial and it has been drawn great attention. Up to now, some materials were reported with adsorption performance, which have been used as adsorbent, such as activated carbon [6], zeolite, alginate bead [7] clay [8] graphene [9], cellulose-based wastes [10] and metal-organic frameworks.

Metal-organic frameworks (MOFs) have attracted widespread attention, due to their high surface areas, ultrahigh porosity, and the easy tunability of their pore size and shape. Thus, it has shown a broad application prospect in terms of gas storage, adsorption, separation, drug delivery [11], proton conduction and catalytic. However, so far, the literature using MOFs to remove the dye materials is less reported, except for the report of protonated ethylenediamine-grafted Cr-terephthalate (MIL-101) ,which has shown high adsorption capacity, rapid uptake and ready regeneration for the MO, and another report is that an iron terephthalate (MOF-235) has been used for the removal of cationic dye methylene blue (MB) from contaminated water via adsorption [12].

Existing literature reports of MOF-5($Zn_4O(BDC)_3$) adsorption are mainly concentrated on the gas phase adsorption, such as CO_2, CH_4, N_2O and N_2[13] and so on. However, the liquid phase adsorption has not been reported. Hence, in this work, we mainly study the liquid adsorption, but the research process of MOF-5 liquid phase adsorption has no obvious effect, so $H_3PMo_{12}O_{40}$ acids was introduced in MOF-5 by using solvothermal method, forming $H_3PMo_{12}O_{40}$/MOF-5 composite. The research results showed that modified material for the cationic dye methylene blue solution had a good adsorption effect, which provided the practical parameters for research reference for the material used for liquid phase adsorption, thus this work has important theoretical significance and application value.

2. EXPERIMENTAL

2.1 Preparation of $H_3PMo_{12}O_{40}$/MOF-5 Adsorbents

Preparation of Keggin $H_3PMo_{12}O_{40}$ acid was synthesized by reflux method as in ref [14-16].

$H_3PMo_{12}O_{40}$/MOF-5 was synthesized by dispersing 0.149 g (0.5 mmol) of $Zn(NO_3)_2{\times}6H_2O$ (Tianjin Tianli Chemical Reagent Co., Ltd. Tianjin, China) and 0.01666 g (0.1mmol) of 1, 4-benzenedicarboxylic acid (Tianjin Guangfu fine Chemical Reagent Institute., Ltd. Tianjin, China) and $H_3PMo_{12}O_{40}$ (0.125 g)were dissolved in 15 mL of N,N-dimethylformamide (DMF) at room temperature. The mixture was transferred into a 25 mL Teflon-lined autoclave, which was sealed and maintained at 393 K for 21 h. After washing, the product was dried at 353 K in a vacuum oven for

12 h and the material obtained was stored in a vacuum dryer for further use in batch experiments.

2.2 Characterization

Functional groups of the samples were analyzed by Fourier transform infrared spectroscopy (FT-IR, Nicolet 5700, America) within the wave range 4,000-500 cm^{-1}. Powder X-ray diffraction (XRD) patterns were collected at a scanning rate of 0.05°/s and 2θ ranging from 5 to 25° on Bruker D8 equipped with Cu Kα radiation (40 kV, 40 mA). Thermogravimetric analyses of the materials were performed using a thermogravimetric analyzer (TGA, Perkin Elmer, America) at a heating rate of 5 K min^{-1} and temperature ranging from 28 °C to 800 °C in a flowing atmosphere of N_2. The surface area (BET), pore volume and pore diameter of the samples were determined from the N_2 adsorption at -196 °C with a Quantachrome ASAP 2020 porosimeter. The samples were degassed at 180 °C under vacuum for 4 h before measurements. The morphology was observed by scanning electron microscope (SEM, S-3400N, Hitachi, Japan). The distribution of element was analyzed by English Dialect Society (EDS, EDAX-X, AMETEK, America).

2.3 Adsorption Experiments

Fixed with dye concentrations from 10 mg/L to 110mg/L. To determine the adsorption capacity at various pH values, the pH of the dye solutions was adjusted with 0.1 mol/L HNO_3 or 0.1 mol/L NaOH aqueous solution. 2 mL of the mixture was taken at predetermined time intervals and then centrifuged at 10000 rpm for 2 min. The final concentration of dye in the solution was analyzed by spectrophotometric method at 664 nm (U-3010, Hitachi, Japan). The adsorption amount q_t ($mg \cdot g^{-1}$) at the time t were calculated as follows:

$$q_t = \frac{(C_o - C_t)V}{m}$$

where Co and Ct are the MB initial and equilibrium concentration. V (mL) is the volume of the MB solution and m (mg) was the mass of adsorbents.

3. RESULTS AND DISCUSSION

3.1 Characterizations of the Materials

The characteristic absorption peaks at 3428.6, 1657.9, 1601.8, 1389.0, 823.4, 750.0 cm^{-1} were attributed to MOF-5 in Figure 1, the FT-IR spectrum of materials, while the correspond peaks of free $H_3PMo_{12}O_{40}$ were consistent with the peaks which has been reported in the literatures [14]. The characteristic peaks were observed at 3430.2, 1656.9, 1386.5, 817.8, 748.5 cm^{-1}, attributed to $H_3PMo_{12}O_{40}$/MOF-5, in addition to retain the characteristic absorption peak of MOF-5 basic skeleton, there also has an obvious band at 877.6 cm^{-1} assigned to ν(Mo-O_b-Mo) of Keggin type phosphomolybdic acid, indicating the Keggin structure of $H_3PMo_{12}O_{40}$ was still preserved after loaded, the phosphomolybdic acid was regarded as a guest molecule within the MOF-5 framework[17].

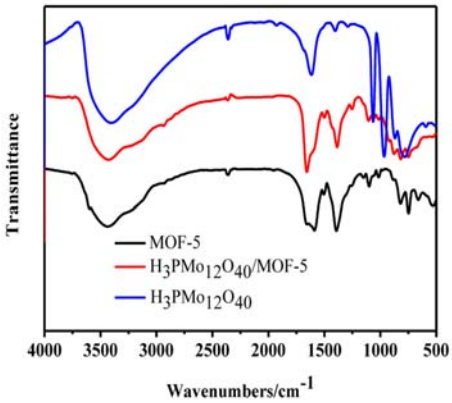

Figure 1. FT-IR patterns of $H_3PMo_{12}O_{40}$, MOF-5 and $H_3PMo_{12}O_{40}$/MOF-5.

The XRD diffraction peaks of $H_3PMo_{12}O_{40}$ were mainly concentrated in $2\theta = 5 \sim 25°$, shown in Figure 2, the characteristic diffraction peaks of the prepared MOF-5[18] were consistent with the peaks which has been reported in the literatures, and the structure of MOF-5 remained unchanged even after adding $H_3PMo_{12}O_{40}$, indicating the fine ordered structure of MOF-5. While detecting the peaks of $H_3PMo_{12}O_{40}$ within the $H_3PMo_{12}O_{40}$ /MOF-5, suggested the $H_3PMo_{12}O_{40}$ was loaded in the channel of MOF-5 or on the surface.

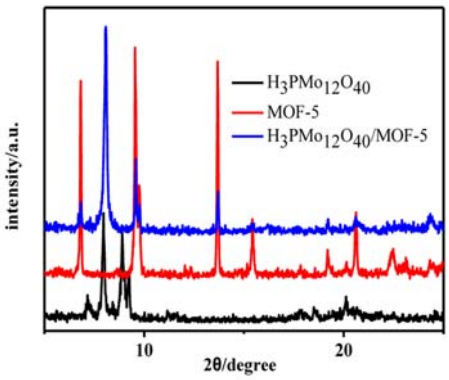

Figure 2. XRD patterns of $H_3PMo_{12}O_{40}$, MOF-5 and $H_3PMo_{12}O_{40}$/MOF-5.

The thermogravimetric curve of MOF-5 and $H_3PMo_{12}O_{40}$/MOF-5 was shown in Figure 3, as the temperature rises, the weight reduces gradually. The process can be calculated for the release of guest molecules in the $H_3PMo_{12}O_{40}$/MOF-5 covered a temperature range from 28 to 250 °C, the temperature range of 28-170 °C was the step which corresponds to the remove of physically adsorbed water as well as crystal water. Above 410 °C, the step was attributed to the collapse of framework, which needed higher temperature than MOF-5, also suggested the $H_3PMo_{12}O_{40}$ was loaded in the channel of MOF-5 or on the surface.

The total sorption capacity of $H_3PMo_{12}O_{40}$/MOF-5 was 107.95 m^2 g^{-1}, which was higher than the pure MOF-5. It was suggested that more pores were present to the composite after the addition of $H_3PMo_{12}O_{40}$ conforming to the results showed in Table 1, where the surface area and pore volume were listed calculated by BJH method. Compared with the pure MOF-5, the surface area and pore volume increased. It can be concluded that the introduction of $H_3PMo_{12}O_{40}$ had a great change to the structure of MOF-5 to form smaller cages [19], which was a favorable factor for enhancing the adsorption performance.

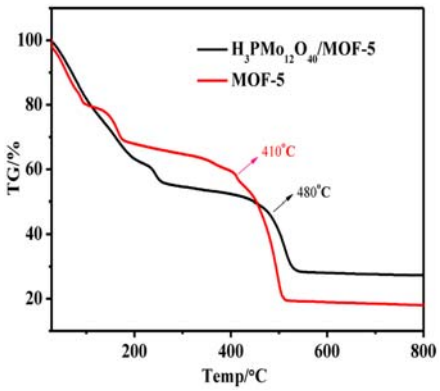

Figure 3. TG-DTG-DTA profile of MOF-5 and $H_3PMo_{12}O_{40}$/MOF-5.

Table 1. Textural property of MOF-5 and $H_3PMo_{12}O_{40}$/MOF-5.

Sample	S_{BET} (m^2g^{-1})	Vtotal (cm^3g^{-1})	D (nm)
MOF-5	58.79	0.062	4.24
$H_3PMo_{12}O_{40}$/MOF-5	107.95	0.069	2.54

S_{BET}: BET surface area.
Vtotal: Total pore volume.
D: Average pore diameter calculated using BJH method.

From Figure 4, $H_3PMo_{12}O_{40}$ appeared as an irregular shape of granular structure. MOF-5 was a cube and its particle diameter was about 20 mm. The pattern of $H_3PMo_{12}O_{40}$ has changed after supported on MOF-5 and the compound appeared as an irregular structure of different shapes and sizes which indicated that $H_3PMo_{12}O_{40}$ were evenly dispersed in the pore of MOF-5.

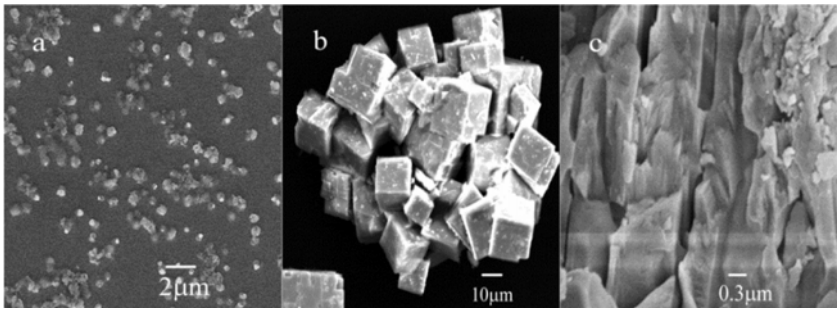

Figure 4. SEM imagines of $H_3PMo_{12}O_{40}$(a), MOF-5(b) and $H_3PMo_{12}O_{40}$/MOF-5(c).

From Figure 5, the absorption peak of main elements of $H_3PMo_{12}O_{40}$/MOF-5 appeared, in which O0Zn0P0Mo included. C was the conductive matrix absorption peak and the atomic molar ratio of P/Mo was about 1:12, which indicated that $H_3PMo_{12}O_{40}$ still maintained its Keggin structure after supported on MOF-5.

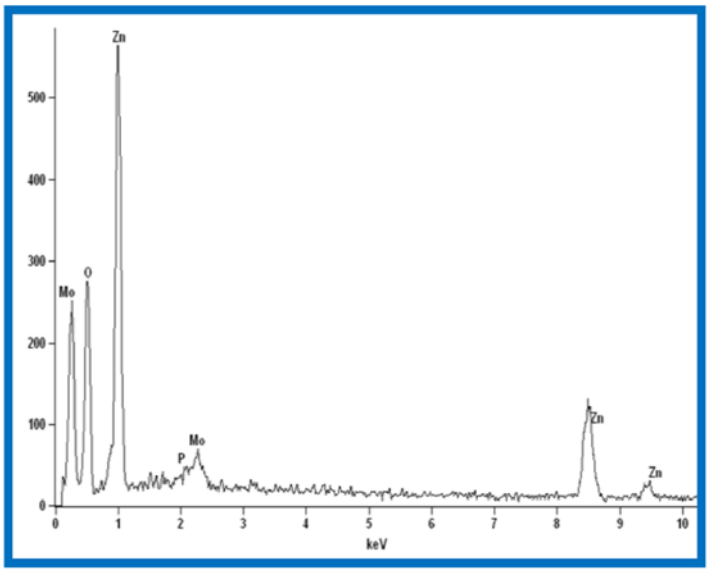

Figure 5. EDS spectra of $H_3PMo_{12}O_{40}$/MOF-5.

3.2 Effect of pH on Methylene Blue Adsorption

As the Figure 6 shows, it was found that the adsorption capacity of $H_3PMo_{12}O_{40}$/MOF-5 reduced with the increase of the solution pH, the pH of dye solution was a very important factor. At lower pH values, hydrogen ion competed with methylene blue cation and hydrogen depressed the ionization of methylene blue [20-21],

The values of the adsorption capability were both largest at pH=2, which indicated that pH=2 benefited MB adsorption and the acidity condition was appropriate to be established as optimal condition for further experiments. and as shown in figure 6 the Zeta-potential was negative and decreased with the increase of pH. At higher pH, both of their adsorption capacities were becoming small and the chloride anion in methylene blue was exchanged with NaOH to have a displacement reaction, which formed NaCl (aq) and MBS+OH (aq). However, the salt of NaCl might result in the deactivation of $H_3PMo_{12}O_{40}$/MOF-5 and eventually decrease the adsorption of MBS+OH (aq) on the $H_3PMo_{12}O_{40}$/MOF-5 [22].

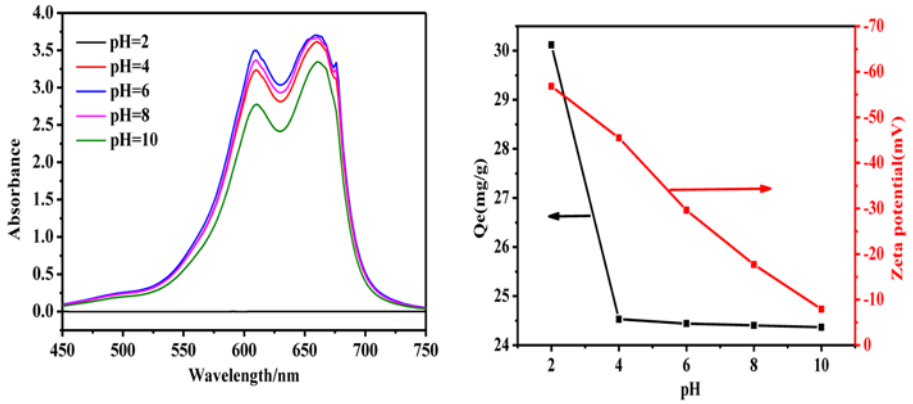

Figure 6. Zeta potentials of $H_3PMo_{12}O_{40}$/MOF-5 at different pH. Adsorption of methylene blue on $H_3PMo_{12}O_{40}$/MOF-5 as a function of pH (Conditions: $H_3PMo_{12}O_{40}$/MOF-5: 1 mg/mL; methylene blue: 30 mg/mL; time: 35 min; temperature: 303K).

3.3 Effect of Initial Concentration Methylene Blue Adsorption

As shown in Figure 7,the adsorption capacity of $H_3PMo_{12}O_{40}$/MOF-5 increased with the increase of initial concentration, the initial concentration of dye solution was a very important factor. The increase of methylene blue concentration could increase onto the surface of $H_3PMo_{12}O_{40}$/MOF-5 and the principal part of methylene blue, which resulted in an increase in the driving force of concentration difference [23] and its adsorption capacity.

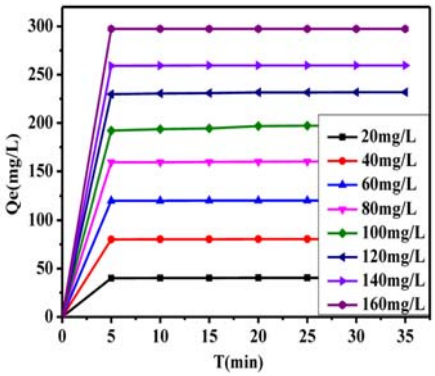

Figure 7. Effect of initial concentration methylene blue adsorption (Conditions: $H_3PMo_{12}O_{40}$/MOF-5:0.5 mg/mL; methylene blue: 20, 40, 60, 80, 100, 120, 140, 160 mg/mL; time: 35 min; temperature: 303 K).

3.4 Effect of Temperature on Methylene Blue Adsorption

As shown in Figure 8, the adsorption amount of methylene blue showed a contrary trend with temperature. As the temperature of $H_3PMo_{12}O_{40}$/MOF-5 increased, the adsorption amount decreased, indicating that the adsorption was an exothermic process. Maybe at higher temperature, the solubility of methylene blue increased, which could also increase the viscosity of solution and the mass transfer resistance between $H_3PMo_{12}O_{40}$/MOF-5 and the dyes. The adsorption of methylene blue on NH_2-OMA has the same experimental phenomenon as what have been described [24].

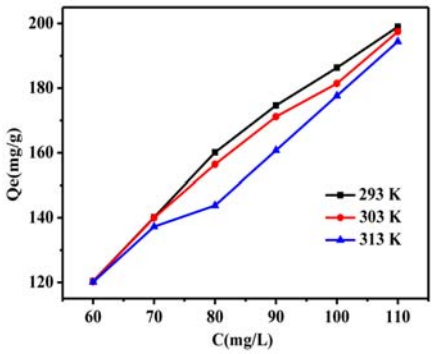

Figure 8. Effect of temperature on adsorption capacities of methylene blue (Conditions: $H_3PMo_{12}O_{40}$/MOF-5: 0.5 mg/mL; methylene blue: 60, 70, 80, 90, 100, 110 mg/mL; time: 240 min; temperature: 293 K, 303 K, 313 K).

3.5 Comparison of Adsorption Ability for Methylene Blue in Pure MOF-5 and $H_3PMo_{12}O_{40}$/MOF-5

Figure 9 shows the effect of $H_3PMo_{12}O_{40}$/MOF-5 and the adsorption of MOF-5 on methylene blue. The adsorption capacity of pure MOF-5 was much smaller than the $H_3PMo_{12}O_{40}$/MOF-5, which has been shown in figure 9. While the concentration of methylene blue solution for 60 mg/L and the value of pH for 2, indicating that the MOF-5 materials can be applied in liquid phase adsorption by using $H_3PMo_{12}O_{40}$ to modify MOF-5, making a more extensive application of MOF-5.

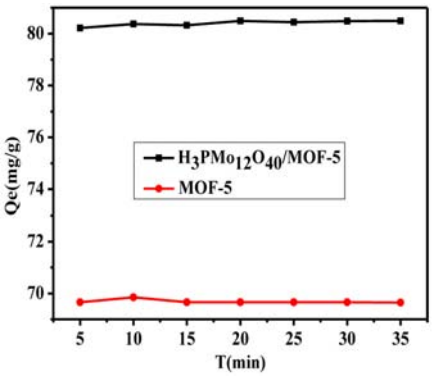

Figure 9. Comparison of adsorption capacity for methylene blue in pure $H_3PMo_{12}O_{40}$/MOF-5 and MOF-5 (Conditions: $H_3PMo_{12}O_{40}$/MOF-5: 0.5 mg/mL; methylene blue: 40 mg/mL; time: 240 min; temperature: 303 K).

3.6 Adsorption of Cationic Dyes

For methyl orange different dyes (20 mL), such as methylene blue, methyl violet, rhodamine B, malachine green, the adsorbent of $H_3PMo_{12}O_{40}$/MOF-5 showed different adsorption capacity with the concentration of 40 mg/L and on the condition of pH 2, shown in Figure 10. The adsorption capacity could reach 80.5 mg/g, 79.4 mg/g, 77.9 mg/g, 79. 8 mg/g and 0.65 mg/g, respectively.

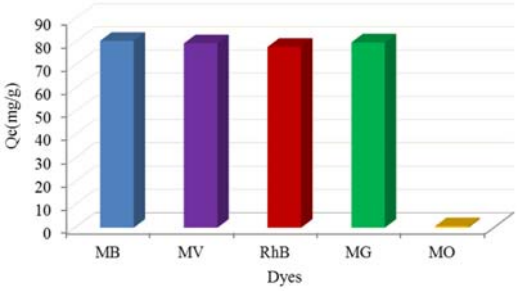

Figure 10. The adsorption of cationic dyes us $H_3PMo_{12}O_{40}$/MOF-5 as a adsorbent (Conditions: $H_3PMo_{12}O_{40}$/MOF-5: 1.0 mg/mL; dyesmethylene blue, methyl violet, rhodamine B, malachine green, methyl orange; concentration: 40 mg/mL; time: 35 min; temperature: 303 K).

3.7 Mechanism of the Adsorption

As the Figure 11 shows, it was found that the adsorption capacity of $H_3PMo_{12}O_{40}$/MOF-5 remained almost constant the increase of the KCl concentration. Therefore, we can conclude that an electrostatic attraction between the positively charged methylene blue molecules and negatively charged $H_3PMo_{12}O_{40}$/MOF-5 was not affected significantly by KCl under the examined condition [25].

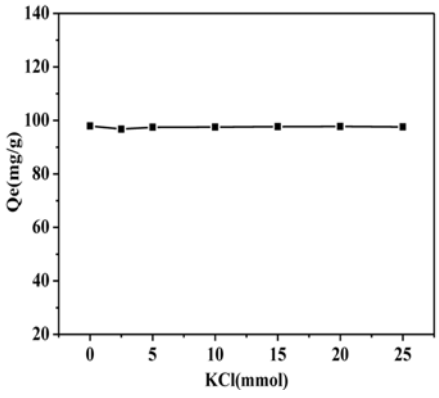

Figure 11. Adsorption of methylene blue on $H_3PMo_{12}O_{40}$/MOF-5 as a function of KCl concentration. (Conditions: $H_3PMo_{12}O_{40}$/MOF-5: 0.5 mg/mL; Methylene blue: 60 mg/L; pH=7; time: 30 min; temperature: 293 K).

4. ADSORPTION ISOTHERMS

On the basis of exploring the influence of temperature, the further research of the two isotherm models can be conducted, respectively the Langmuir isotherm and the Freundlich isotherm, were used to describe the adsorption progress and mechanisms. The equation of Langmuir isotherm[26] model could be expressed as follows:

$$\frac{C_e}{q_e} = \frac{1}{q_m} C_e + \frac{1}{q_m K_L}$$

where q_e and q_m(mg/g) were respectively called the adsorption capacity at equilibrium and the maximum per unit adsorption amount of $H_3PMo_{12}O_{40}$/MOF-5, *Ce*(mg/L) was the equilibrium concentration of MB, K_L(L/mg) called the equilibrium constant of Langmuir model. The plot of *Ce* vs. *Ce*/*q* yielded a straight line was shown in figure 12, which suggested that the adsorption of MB onto $H_3PMo_{12}O_{40}$/MOF-5 was confirmed to the Langmuir isotherm model, the calculated correlation parameters was shown in Table 2.

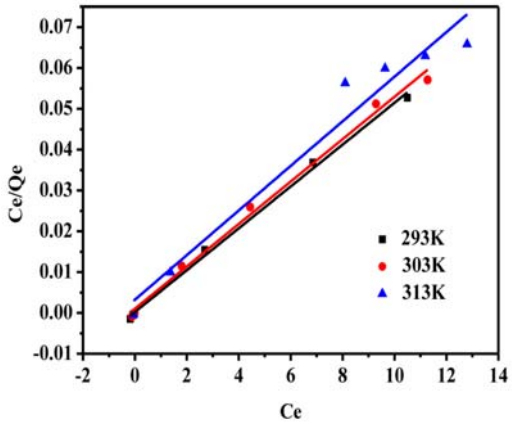

Figure 12. Langmuir isotherm of methylene blue adsorption onto $H_3PMo_{12}O_{40}$/MOF-5.

Table 2. Isotherm parameters for removal of methylene blue by $H_3PMo_{12}O_{40}$/MOF-5 at different temperature.

Adsorption	Constant	293K	303K	313K
Langmuir	Q_m(mg/g)	194.93	192.31	183.15
	K_L(L/mg)	0.00135	5.10	1.69
	R_L	0.8974	0.0024	0.00721
	R^2	0.9987	0.9972	0.9812
Freundlich	K_F(mg/g)	13.77	13.54	13.19
	n	10.89	8.81	8.36
	R^2	0.9761	0.9639	0.7609

As a separation term, a dimensionless constant, R_L could be expressed the basic characteristics of Langmuir isotherm, was introduced as follows[27]:

$$R_L = \frac{1}{1 + bC_0}$$

Where C_0 (mg/L) was the initial concentration of MB. The values of R_L could be suggested the ability of relevant adsorption isotherm, which was unfavorable (R_L>1), favorable (0<R_L<1), while irreversible (R_L= 0) or linear (R_L=1).

The R_L values of the adsorption of MB onto $H_3PMo_{12}O_{40}$/MOF-5 were respectively 0.8974, 0.0024 and 0.00721, on the conditions of 293 K303 K313 K, which indicated this process was favourable.

Regarded as an empirical equation[28], the Freundlich isotherm was generally represented by:

$$\ln q_e = \frac{1}{n} \ln C_e + \ln K_F$$

Where K_F is a Freundlich constant, confirmed the adsorption capacity, while 1/n indicated the adsorption intensity. And the related parameters calculated were shown in Table 2.

Embraced the parameters of the two models. It was quite clear that the adsorption process was fitter for the Langmuir isotherm model than another one. What's more, there also exists the corresponded literature which had reported[28] the Langmuir isotherm model.

5. ADSORPTION KINETICS

There were two kinetic models, pseudo-first-order and pseudo-second-order, respectively, which were used to fit experimental data to further evaluate the mechanism of this adsorption.

5.1 The Pseudo-first-order Model

Simple as a dynamic adsorption analysis equation, Langmuir equation [29] could be expressed as follows:

$$\frac{dq_t}{d_t} = k_1(q_e - q_t)$$

Where K_1 (min^{-1}) was the adsorption rate constant of $H_3PMo_{12}O_{40}$/MOF-5, q_e and q_t (mg/g) respectively represent the capacity of adsorption at equilibrium state and at time t (min). While the value of t is 0, q_t=0, and the t value is equal to t, q_t=q_t, therefore the above equation can be transformed into the type ,which can be represented as follows:

$$\ln(q_e - q_t) = \ln q_e - k1t$$

k_1 (min^{-1}) called the Lagergren rate

constant of adsorption, can be calculated from the slope of the plot of t v.s In (q_e-q_t) in Figure 13.

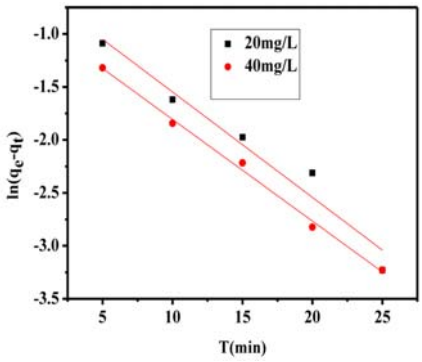

Figure 13. The pseudo first-order model for adsorption of methylene blue onto $H_3PMo_{12}O_{40}$/MOF-5 curves at different initial concentration.

The linear correlation coefficient R^2 values determined by pseudo-first-order model of $H_3PMo_{12}O_{40}$/MOF-5 reached up to 0.9804 and 0.9979 on different initial concentrations of 20mg/L and 40mg/L. However ,the experimental q_e values was totally less closer to the calculated ones of the pseudo-second-order kinetic model which were shown in Table 3, which demonstrated that the adsorption of MB onto $H_3PMo_{12}O_{40}$/MOF-5 was not consistent with the pseudo-first-order kinetic model and the adsorption process was not controlled by diffusion [30].

5.2 The Pseudo-second-order Model

The pseudo-second-order model [29] was commonly expressed in linear form as follows:

$$\frac{t}{q_t} = \frac{1}{k_2 q_e^2} + \frac{1}{q_e} t$$

Where K_2 (g/(mg□ min)) is the pseudo-second-order model adsorption rate constant of $H_3PMo_{12}O_{40}$/MOF-5. As shown in Figure 14 the experimental q_e values were consistent with the calculated ones, shown in Table 3, and the correlation coefficient R^2 values of pseudo-second-order model were equal to 1, showed the absorption of MB on $H_3PMo_{12}O_{40}$/MOF-5 fitted the pseudo-second-order model, controlled by chemisorption process[31].

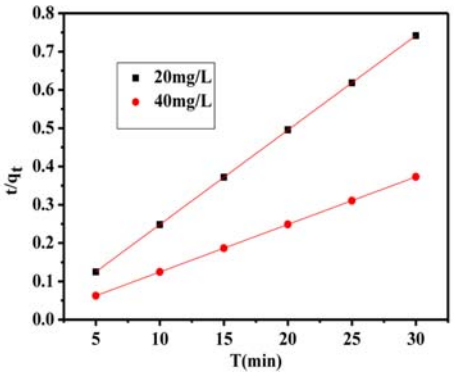

Figure 14. The pseudo second-order model for adsorption of methylene blue onto $H_3PMo_{12}O_{40}$/MOF-5 curves at different initial concentration.

Table 3. The parameters of pseudo-first-order and pseudo-second-order adsorption kinetics model in different initial concentration.

Kinetics model	Initial concentration (mg/L)	$Q_{e,exp}$ (mg/g)	$Q_{e,cal}$ (mg/g)	$K_1(min^{-1})$; $K_2(g/(mg\cdot min))$	R^2
Pseudo-first-order	20	40.47	-1.5036	0.09947	0.9804
model	40	80.49	-2.3445	0.096	0.9979
Pseudo-second-order	20	40.47	40.54	0.3803	1
model	40	80.49	80.52	0.0000495	1

6. THERMODYNAMIC PARAMETERS

The adsorption experiment of MB on $H_3PMo_{12}O_{40}$/MOF-5 with the temperature of 293K303K and 313K, was used to explore adsorption equilibrium constants K_L, the gibbs free energy (ΔG^0), enthalpy chan ge (ΔH^0) and entropy change (ΔS^0), which were expressed by the following equations:

$$K_L = \frac{q_e}{C_e}$$

$$\Delta G = -nRT$$

$$\ln K_L = \frac{\Delta S^0}{R} - \frac{\Delta H^0}{RT}$$

Where the constant R is 8.3145 J mol^{-1} K^{-1}, T named temperature(K).the ΔH and ΔS can be obtained from the slope and intercept of the plot of 1/T vs lnk_L, and these thermodynamic parameters were listed in Table 4, respectively.

Table 4. The thermodynamic parameters of adsorption methylene blue onto $H_3PMo_{12}O_{40}$/MOF-5.

Adsorbates	ΔG (KJ/mol)			ΔH (KJ/mol)	ΔS ($J\cdot mol^{-1}K^{-1}$)
	293K	303K	313K		
MB	-8.4590	-8.7881	-8.2169	-11.86	-11.12

The relevant data indicated that the adsorption process was a spontaneous and exothermic process because of $\Delta G < 0$ and $\Delta H < 0$, which could further illustrate the experiment result.

7. CONCLUSION

The quite efficient adsorption of methylene blue dye in aqueous solution on $H_3PMo_{12}O_{40}$/MOF-5 was studied. The maximum adsorption capacity was 194.93 mg/g, and showed good adsorption effect to several other cationic dyes, such as methyl violet, rhodamine B, malachite green, therefore it had potential industrial application value. It was benefit to the absorption of MB on $H_3PMo_{12}O_{40}$/MOF-5 with the decreasing of temperature and pH, which could also be proved by thermodynamic parameters. This adsorption process was well fitted by Langmuir isotherms model and pseudo-second-order kinetic model, the relevant data indicated that the adsorption process was a spontaneous and exothermic process because of $\Delta G < 0$ and $\Delta H < 0$, which could further illustrate the experiment result.

ACKNOWLEDGMENTS

This work was financially supported by the Supported by National Natural Science Foundation of China (No. 21171053) Natural

Science Foundation of Hubei Province (No.2014CFA131) and Postgraduate Innovation Scientific Research Foundation of Hubei Normal University (No. 20160107).

REFERENCES

[1] Rebane R., Leito I., Yurchenko S. and Herodes K., *J. Chromatogr. A*, 2010; **1217**: 747-757. DOI 10.1016/j.chroma.2010.02.038.

[2] Liang M., Xu W., Cai F., Chen P., Peng B., Chen J. and Ming C., *J. Phys. Chem. C.*, 2007; **111**: 4465-4472. DOI 10.1021/jp067930a.

[3] Zhang J., Gondal M.A., Wei W., Zhang T., Xu Q. and Shen K., *J. Alloys Compd.*, 2012; **530**: 107-110. DOI 10.1016/j.jallcom.2012.03.104.

[4] Chen Z., Adil K. and Weselinski L.J., *Mater. Chem. A*, 2015; **3**: 6276-6281. DOI 10.1039/c4ta07115h.

[5] Crini G., *Bioresour. Technol.*, 2006; **97**: 1061-1085. DOI 10.1016/j.biortech.2005.05.001.

[6] Banat I.M., Nigam P., Singh D. and Marchant R., *Bioresour. Technol.*, 1996; **58**: 217-227. DOI 10.1016/S0960-8524(96)00113-7.

[7] Ma J.F., Huang D.Q., Zou J., Li L.Y., Kong Y. and Komarneni S., *J. Porous Mater.*, 2015; **22**: 301-311. DOI 10.1007/s10934-014-9896-2.

[8] Rocher V., Siaugue J.M.,Cabuil V. and Bee A., *Water Res.*, 2008, **42**: 1290-1298. DOI 10.1016/j.watres.2007.09.024.

[9] Oztekin N., Alemdar A., Gungor N. and Bedia E.F., *Mater. Lett.*, 2002; **55**: 73-76. DOI 10.1016/S0167-577X(01)00622-X.

[10] Iturbe E.J., Andrade M.J., Gómez R., and Rodríguez G.V., *Mater. Lett.*, 2015; **142**: 75-79. DOI 10.1016/j.matlet.2014.11.149.

[11] Annadurai G., Juang R.S. and Lee D.J., *J. Hazard. Mater.*, 2002; **92**: 263-274. DOI 10.1016/S0304-3894(02)00017-1.

[12] Sun C.Y., Qin C., Wang X.L. and Su Z.M., *Exper. Opin. Drug Deliv.*, 2013; **10**: 89-101. DOI 10.1517/17425247.2013.741583.

[13] Haque E., Jun J.W. and Jhung S.H., *J. Hazard. Mater.*, 2011; **185**: 507-511. DOI 10.1016/j.jhazmat.2010.05.047.

[14] Dipendu S., Zongbi B., Feng J. and Deng S.G., *Environ. Sci. Technol.*, 2010; **44**: 1820-1826. DOI 10.1021/es9032309.

[15] Li S.J., Peng Q.P., Chen X.N., Wang R.Y., Zhai J.X., Hu W.H., Ma F.J., Zhang J. and Liu S.X., *J. Solid State Chem.*, 2016; **243**: 1-7. DOI 10.1016/j.jssc.2016.08.003.

[16] Li S.J., Zhang F.Y., Peng Q.P., Chen X.N., Wang R.Y., Wang Z.F., Ma F.J., Zhao Q.Y. and Wei M.L., *J. Coord. Chem.*, 2016; **69**: 425-432. DOI 10.1080/00958972.2016.1138106.

[17] Sun C.Y., Liu S.X., Liang D.D., Shao K.Z., Ren Y.H. and Sun Z.M, *J. Am. Chem. Soc.*, 2009; **131**: 1883-1888. DOI 10.1021/ja807357r.

[18] Park D.R., Song J.H., Lee S.H., Song S.H., Kim H., Jung J.C. and Song I.K., *Appl. Catal. A-Gen.*, 2008; **349**: 222-228. DOI 10.1016/j.apcata.2008.07.042.

[19] Liu Y.W., Liu S.M., He D.F., Li N., Ji Y.J., Zheng Z.P., Luo F., Liu S.X., Shi Z. and Hu C.W., *J. Am. Chem. Soc.*, 2015; **137**: 12697-12703. DOI 10.1021/jacs.5b08273.

[20] Panella B. and Hirsche M., *Adv. Mater.*, 2005; **7**: 538-541. DOI 10.1002/adma.200400946.

[21] Gupata K.C., Majeti N.V. and Ravi K., *Appl. Polym. Sci.*, 2001; **80**: 639-649. DOI 10.1002/1097-4628(20010425)80:4<639.

[22] Senthilkumaar S., Varadarajan P.R., Porkodi K. and Subbhuraam C.V., *J. Colloid Interface Sci.*, 2005; **284**: 78-82. DOI 10.1016/j.jcis.2004.09.027.

[23] Lin S., Song Z., Che G., Ren A., Li P., Liu C.B. and Zhang J., *Microporous Mesoporous Mater.*, 2014; **193**: 27-34. DOI 10.1016/j.micromeso.2014.03.004.

[24] Ozer A. and Dursun G., *J. Hazard. Mater.*, 2007; **146**: 262-269. DOI 10.1016/j.jhazmat.2006.12.016.

[25] Wei W., Lu L.J., Xie H.J., Zhang Y.F., Bai X., Gu L., Da R. and Liu X.Y., *J. Mater. Chem. A.*, 2015; **3**: 4314-4322. DOI 10.1039/C4TA06444E.

[26] Gan Y.Q., Tian N., Ma L.L., Wang W.W., Yang C., Zhou Q.X. and Wang Y.X., *J. Porous Mater.*, 2015; **22**: 147-155. DOI 10.1007/s10934-014-9881-9.

[27] Langmuir I., *J. Am. Chem. Soc.*, 1918; **40**: 1361-1403. DOI 10.1021/ja02242a004.

[28] Hameed B.H., *J. Hazard. Mater.*, 2008; **154**: 204-212. DOI 10.1016/j.jhazmat.2007.10.010.

[29] Malik P.K., *Dyes Pigm.*, 2003; **56**: 239-249. DOI 10.1016/S0143-7208(02)00159-6.

[30] Ho Y.S., Chiu W.T. and Wang C.C., *Bioresour. Techonl.*, 2005; **96**: 1285-1291. DOI 10.1016/j.biortech.2004.10.021.

[31] Chen S.H., Zhang J., Zhang C.L., Yue Q.Y., Li Y. and Li C., *Desalination*, 2010; **252**: 149-156. DOI 10.1016/j.desal.2009.10.010.